中國機械工程學刊第四十五卷第五期第 453~460 頁(民國一百一十三年)
Journal of the Chinese Society of Mechanical Engineers, Vol.45, No.5, pp453~460 (2024)

# Deep Learning-Based Welding Defect Identification Device: A Comparative Analysis and Superiority Assessment in Industrial Applications

Chia-Hung Lai

***Keywords*** ― CNN model, nondestructive testing, welding defects, image recognition.

## ABSTRACT

Welding has broad applications. Nondestructive testing plays a crucial role in welding inspection. Every weld must be assessed for quality and the absence of defects, but such assessments must be done manually by an experienced operator. Thus, we formulated a deep-learning-based device that automatically conducts such assessments. We trained Welding Defects Net (WDNet) model with a small amount of images and adjusted the depth of convolutional layers and pooling layers during training. We also competitively evaluated several deep learning models for welding defect identification, the first in the literature to do so. In evaluation experiments, our device had accuracy rates as high as 97.8%, outperforming Visual Geometry Group 16 (VGG-16) and Residual Neural Network 50 (ResNet50) demonstrating promise for use in industrial settings.

## INTRODUCTION

Welding has a wide range of applications and can be adapted for use with materials of a diverse range of shapes. Welding inspections are crucial to ensure the structural integrity (and thus, safety) of the weld. However, because such inspections are traditionally done manually by an experienced operator, assessments cannot be done on the fly and misjudgments may occur. Researchers have thus formulated machine vision approaches, particularly convolutional neural network (CNN)-based ones, for welding assessment.

*Paper Received December 2023. Revised March 2024. Accepted May 2024. Author for Corresponding: Chia-Hung Lai*

* *Assistant Professor, Department of Intelligent Automation Engineering, National Chin-Yi University of Technology, Taiwan, 411030, ROC.*

Methods for welding defect detection can be destructive or nondestructive. Destructive detection methods are used in the testing and development of new products. Nondestructive detection methods are used for routine welding inspections and have the advantage of preserving the structural integrity of a workpiece. CNNs have performed well in industrial machine applications (Xiao, 2022). Lin (2020) used the support vector machine and artificial fish-swarm algorithms to inspect ball bearings to improve accuracy. Jian (2019) conducted domain testing on spindle displacement using a general regression neural network and found that the maximum error of this method was less than 1°C. Wang (2022) predicted turning precision using XGBoost and reduced the cost of predicting machining errors. Wang (2021) predicted the nonlinear behavior in a robotic arm by using impact recognition and machine learning, achieving very high accuracy.

Image recognition technologies are widely applied in welding inspection applications. Typically, these technologies involve the use of trained models in the detection of welding defects (Zapata, 2011; Yaacoubi, 2022). In contrast to traditional approaches where trained models are often not directly integrated into practical applications to form tangible expert systems, our proposed method introduces a novel welding image recognition system utilizing CNN technology, named Welding Defects Net (WDNet). We established a welding image recognition system that preprocesses images and extracts welding defect features. Trained models are then employed to detect welding defects. We compared our method with VGG-16 and ResNet50. We constructed a welding defect detection setup by integrating our image recognition system into a physical device. The primary contributions of this research are as follows:

1. Developed a welding defect detection system that rapidly and effectively detects welding defects.
2. Identification of weld bead defects using instance-based deep learning models.
3. Developed a model that outperforms most existing models in weld bead detection.
4. Annotated of 1131 welding defect images.

# LITERATURE REVIEW

**Welding Defect Detection**

Artificial intelligence can be used to rapidly detect defects (Zeba, 2021). Yu (2021) investigated arc welding molten pool recognition, segmenting molten pools using U-Net, annotating molten pool images, and training a robust CNN that was reliable under various current and welding speed conditions. Lü (2022) examined weld seam recognition, fine-tuning Alexnet, acquiring images, performing transfer learning, and developing a highly accurate method. Gantala (2021) investigated artificial intelligence–assisted automatic identification of welding defects, performing finite element verification, batching finite element weld data creation, training weld data sets, extracting noise into simulated weld images, performing training using a CNN, and developing a method that can effectively improve the reliability and efficiency of welding quality control. Wang (2021) investigated the use of deep learning, data collection, image preprocessing, and CNN model training and testing for welding defect detection and developed a continuous input recurrent neural network model that uses a CNN to automatically extract image features and a recurrent neural network that has sequential processing capability and improves prediction accuracy. Lei (2021) investigated the multisensor tracking of tube-sheet TIG welding seams in motion. Through visual inspection, image tracking, and working principles (calibration and tracking), good control of tube core errors and better welds were achieved. Liu (2022) developed an accurate X-ray-based welding image recognition system. Nacereddine (2019) classified welding defects by using a Gaussian mixture model with a 96% accuracy rate.

**Convolutional Neural Network**

CNNs have been widely used in image recognition applications. Volume muscle neural networks have considerable advantages in two-dimensional image recognition and classification applications (Paoletti, 2018). Su (2018) classified malware using an image recognition system that incorporated a distributed denial-of-service filter and an image classification and detection neural network. The system accurately classified malware. Shang (2018) developed a CNN image classification system for use with rail surface images. The system involved image preprocessing, removal of false edge points, and classification, was robust, and achieved accurate detection results.

Fujiyoshi (2019) examined image recognition for autonomous driving, object detection, image classification, and image recognition. Their findings revealed that deep learning-based image recognition methods had a more pronounced impact compared to object recognition methods based on deep learning. Islam (2018) investigated the use of deep learning image recognition and corroborated the use of CNN for image recognition applications. Miao (2021) used a CNN for image recognition to inspect welding defects. The CNN quickly and accurately extracted weld positions and edge division areas. Hu (2022) improved the extraction range of weld features and reduced noise interference by using a CNN and performed X-ray weld defect identification, achieving improvements in accuracy. Xiao (2022) used a CNN to identify spot welding surfaces. The CNN has a fairly high accuracy rate. Yang (2020) proposed a CNN for image recognition in a laser welding application. The CNN has an accuracy rate as high as 95%.

**Image Detection**

Subtle changes in the picture compromise accuracy in image recognition, and nonlinear models accounting for image variability can be used to remedy this problem (Keysers, 2007). Image recognition models require large training sets. Augmenting raw image data through the Internet can greatly reduce the need for training data (Han, 2018). Pan (2020) used MobileNet for the identification and classification of welding defect images. Welding defects were classified using TL-MobileNet, and the model was found to be accurate in evaluation experiments.

Joutou (2009) developed an image recognition system, performing feature extraction and multiple kernel learning. The system accurately performs food classification tasks. Al-Maadeed (2018) developed an image recognition system that involves the modification of two-dimensional feature points and that can be integrated into cars. The system combines scale-invariant feature conversion, multiscale Harris, and multiscale Hessian and achieves good recognition. Cusano (2017) identified aircraft mechanical parts using an image recognition system that helps maintenance personnel carry out aircraft maintenance. Ai (2023) used image recognition and deep learning methods to predict the weld seam area in laser welding. The methods were robust and accurate. Zhang (2022) performed transfer learning to develop an image recognition system for welding defects. Compared with traditional machine learning methods and deep learning models, the developed system has good robustness and generalization. Zhao (2022) used deep learning to develop an image recognition system for welds, segmented images by using a neural network, and achieved excellent results. Chen (2022) performed feasibility calculations, preselection, and reinspection and developed a welding robot that achieved excellent effects in terms of errors and omissions in the identification and positioning of welding fillets.

# METHODOLOGY

We designed a set of welding defect detection models that employ CNNs. The images used in the present study were captured by researchers at a factory.

The captured images were examined to confirm the presence of welding defects and stored in a database. The models were then trained and tested using this database, and the quality of welds was assessed. We compared the designed models with VGG-16 and ResNet50. We compiled a training data set using images of welded joints. Our goal was to train the models and employ them to detect welding defects in joints.

In Taiwan, welding inspections proceed in two stages. In the first stage is visual inspection after an assessment, and in the second stage is destructive testing. The CNN model proposed in this study was employed for the first stage. The model is based on codes on plates. Our proposed a large volume of welds to be inspected, initial surface inspection is necessary to distinguish between good and bad welds. Due to the difficulty in training welding inspectors and the high demand for welding inspectors, training a model with a small number of images can effectively reduce training costs. The inspection equipment developed in this study in figure 1 which include serval parts, consists of a base 1, a positioning device 11, four lighting devices 2, and a camera 3. A welding seam to be inspected is placed in the middle of the base, within the four positioning devices. The lighting devices are placed around the welding seam to provide illumination; the illumination conditions approximate those in real-world inspection. The weld bead length is 150 mm. The image size is 256 × 256 pixels. The image capture device is KEYENCE IV3-G120. An overhead camera captures the state of the welding seam for recognition (Figure 1). The welding parameters used in this experiment are shown in Table 1.

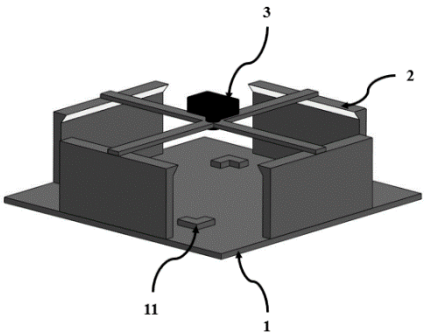


Figure 1 Model Inspection Illustration

Table 1. Welding parameters and conditions.

| | |
|---|---|
| Welding methods | Arc welding |
| Materials | SS400 carbon steel plates |
| Pre-bending angle | 10° |
| Current size | 200A |
| Welding time | 60sec |
| Cooling time | 120sec |

**Image Preprocessing**

First, the collected images were labeled. We categorized the collected images into good shielded metal arc weld beads and bad shielded metal arc weld beads (Figures 2 and 3). We augmented the original data set by horizontally or vertically flipping the images. This expansion led to the data set's size being increased by a factor of one to two times its initial size. Additionally, contrast adjustments were applied to the images in the original data set, both increasing and decreasing contrast, resulting in a further data set expansion of one to two times the initial size. Ultimately, we standardized the images into matrices with dimensions of 64 × 64 × 3 pixels. This standardization enabled the images to be output on the basis of preceding classifications. The images were resized into matrices with dimensions of 64 × 64 pixels, taking into account their RGB color format. As a result, the images were represented as matrices with dimensions of 64 × 64 × 3 pixels. The images were automatically recognized as RGB. Subsequently, both the images and corresponding labels were prepared for output. The quantity of images in the data set is illustrated in Table 2.

Table 2. Data set sizes.

| | Count |
|---|---|
| Train Database | 1000 |
| Test Database | 300 |
| Verify Database | 155 |

Figure 2. Good shielded metal arc weld bead.

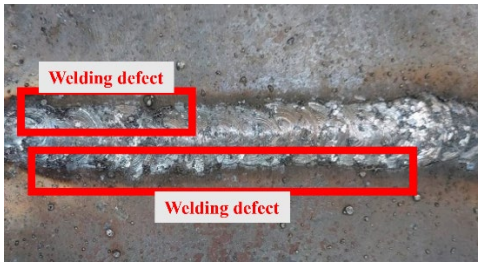


Figure 3. Bad shielded metal arc weld bead.

**VGG-16 Model Architecture**

The VGG-16 comprises three blocks, each composed of convolutional layers followed by pooling layers. The first block includes two convolutional layers (3 × 3 × 64) paired with a pooling layer (2 × 2 × 64). The second block comprises two convolutional layers (3 × 3 × 128) paired with a pooling layer (2 × 2 × 128). The third block, which must be stacked twice, consists of two convolutional layers (3 × 3 × 512) paired with a pooling layer (2 × 2 × 512). The convolutional layers all have a filter size of 3 × 3, and the pooling layers have a filter size of 2 × 2. The number of epochs is 50. The architecture of VGG-16 is illustrated in Figure 3.

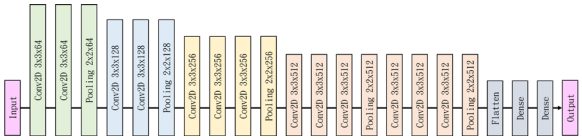


Figure 4. VGG-16 model architecture.

VGG-16 employs very small (3 × 3) convolutional layer filter sizes for deep learning (Simonyan, 2014). However, extended training of VGG-16 often results in a reduction in the learning rate, leading to the problem of vanishing gradients.

**ResNet50 Model Architecture**

ResNet50 has several key components. It begins with an initial convolutional layer using a (7 × 7 × 64) convolutional kernel for the first block. The second block is formed by combining three convolutional kernels (1 × 1 × 64, 3 × 3 × 64, and 1 × 1 × 256). This block is stacked three times. The third block contains three convolutional kernels (1 × 1 × 128, 3 × 3 × 128, and 1 × 1 × 512) and is stacked four times. The fourth block contains three convolutional kernels (1 × 1 × 256, 3 × 3 × 256, and 1 × 1 × 1024) and is stacked six times. The fifth block contains three convolutional kernels (1 × 1 × 512, 3 × 3 × 512, and 1 × 1 × 2048) and is stacked three times. The network includes supplementary layers, such as a pooling layer and fully connected layers. Overall, ResNet50 has a total of 50 layers. The number of epochs is 50. The architecture of ResNet50 is illustrated in Figure 4.

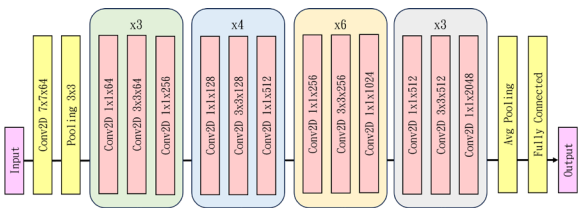


Figure 5. ResNet50 model architecture.

Improvements in model accuracy are not associated with the depth of model training. Deeper models are more susceptible to the vanishing gradient problem (Renjun, 2022). ResNet50 employs identity mapping. When training the next layer, only the residual function needs to be trained. When the dimensions of convolutional layers are the same, using residual functions simplifies the deep learning network, facilitating the training of deep learning models (He, 2016). The calculation of the residual function is illustrated as follows:

$$y = F(x) + x \tag{1}$$

When the dimensions of convolutional layers are different. $W$ represents a convolutional layer. $X$ is used to adjust the intermediate dimensions. The calculation of the adjusted residual function is as follows:

$$y = F(x) + Wx \tag{2}$$

**WDNet Model Architecture**

CNNs primarily consist of convolutional, pooling, and fully connected layers. When these layers are stacked together, they form a CNN module. The convolutional layer is the first layer of the CNN, and multiple convolutional layers and pooling layers can be connected behind the convolutional layer. With each additional layer, the complexity of the CNN module and the accuracy of detecting and predicting objects increase.

Where the convolutional layer is responsible for extracting image features, different features are extracted from the input image. These extracted features are regarded as filters, and the mathematical operation of convolution is performed on the input of the image and the filter of a specific size. Calculated results are transmitted to the next layer. The pooling layer reduces the size of the convolutional feature map and preserves extracted image features by using the convolutional layer. The pooling layer is used to reduce the number of operations to improve the operational efficiency of the CNN and prevent over-learning.

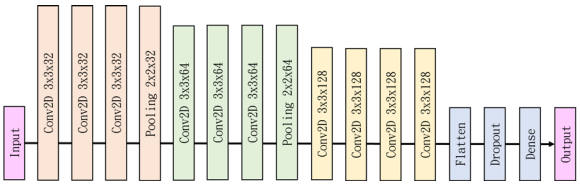


Figure 6. WDNet model architecture.

The CNN in this study consists of three modules. The first module contains four convolutional kernels with dimensions of 3 × 3 × 32 accompanied by a pooling layer of size 2 × 2 × 32. The second module contains four convolutional kernels with dimensions of 3 × 3 × 64 and a pooling layer of size 2 × 2 × 32.

The third module contains four convolutional kernels with dimensions of 3 × 3 × 128 paired with a pooling layer of size 2 × 2 × 32. The architecture of our proposed model is illustrated in Figure 6.

## RESULTS

We conducted welding defect recognition. Accuracy indicates the proportion of correctly identified welding defects. We employed WDNet and measured accuracy rates at epochs 10, 30, 50, 100, and 200 (Table 3).

Table 3. Accuracy of WDNet at different epochs.

| Epochs | 10 | 30 | 50 | 100 | 200 |
|---|---|---|---|---|---|
| *Accuracy* | 68.5 % | 93.2 % | 96.6 % | 97.5 % | 97.8 % |

The process by which we trained WDNet model is illustrated in Figures 6 through 10. At 10 epochs of training, the loss decreased considerably (Figure 6). By the 30th epoch, the loss decreased from 0.7 to 0.1 (Figure 7). At the 50th epoch, the loss increased before decreasing (Figure 8). After approximately the 60th epoch, the loss plateaued (Figure 9). After the 100th epoch, the loss fluctuated slightly before stabilizing (Figure 10).

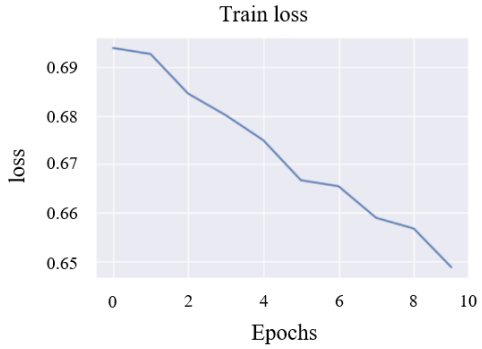


Figure 7. Training and loss results at 10 epochs.

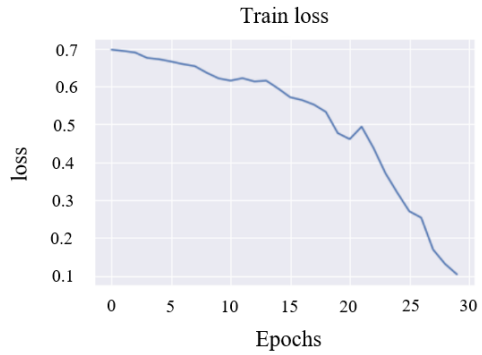


Figure 8. Training and loss results at 30 epochs.

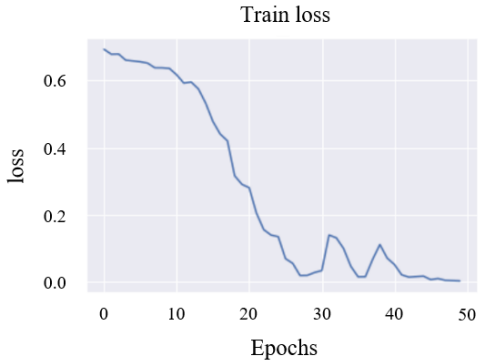


Figure 9. Training and loss results at 50 epochs.

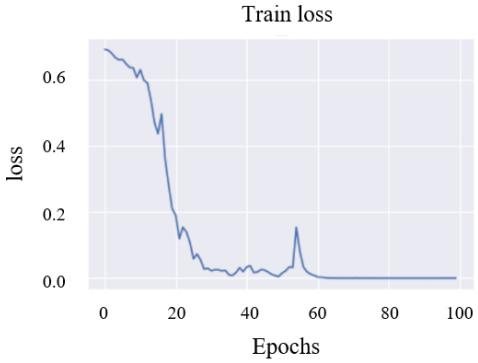


Figure 10. Training and loss results at 100 epochs.

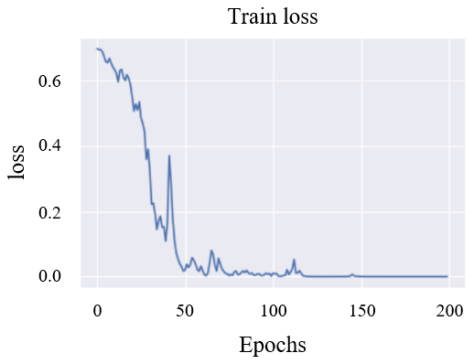


Figure 11. Training and loss results at 200 epochs.

Accuracy is a simple metric of model performance and is defined in Equation (3). The F-measure is often used to represent the importance of precision in image recognition and is defined in Equation (4). Precision and Recall are defined in Equations (5) and (6), respectively. The F-measure is based on the numbers of true positives (*TP*), false negatives (*FN*), false positives (*FP*), and true negatives (*TN*), where a positive instance was defined as the presence of a fault.

$$Accuracy = \frac{TP+TN}{TP+FP+FN+TN} \quad (3)$$

$$F-measure = 2 \times \frac{precision \times recall}{precision + recall} \quad (4)$$

$$Precision = \frac{TP}{TP+FP} \quad (5)$$

$$Recall = \frac{TP}{TP+FN} \quad (6)$$

WDNet model was evaluated against VGG-16 and ResNet50. WDNet model had the highest accuracy at 97.8%, higher than VGG-16's accuracy of 94.1% and slightly higher than ResNet50's accuracy. WDNet model had the second-best F-measure at 97.7%, higher than VGG-16's 94% but slightly lower than ResNet50's 97.8%. WDNet model had the second-best precision at 96.7%, higher than VGG-16's 91.9% but lower than ResNet50's 99.3%. WDNet model had the best recall at 98.6%, higher than VGG-16's 91.9% and ResNet50's 96.4%.

In general, WDNet model is feasible. The accuracy results of the three models are shown in Table 4.

Table 4. Accuracy of proposed CNN model, VGG-16, and Resnet50.

| | WDNet | VGG-16 | Resnet50 |
|---|---|---|---|
| *Accuracy* | 97.8% | 94.1% | 97.8% |

## CONCLUSIONS

We formulated a welding defect detection device that accurately identifies defects through images captured by a camera. In particular, our method, WDNet effectively extracts irregular features from images of welds. Through images captured by the camera within the model, it identifies welding defects and accomplishes the task of defect detection. After validation, this approach has achieved high accuracy, demonstrating the effectiveness of the proposed model in extracting irregular features of welds. Upon comparison with the VGG-16 and ResNet50 models, our model has proven to outperform most existing approaches. It performed well against VGG-16 and ResNet50 in evaluation experiments.

While the model proposed in this study has achieved promising results in welding defect detection, this remarkable research outcome underscores the potential of the method. However, during the data collection process, external factors such as welding slag can introduce numerous uncontrollable interferences due to environmental influences. In the future, continuous research can be conducted in the field of welding inspection to develop new methods that could more effectively identify welding defects within the welding recognition domain. Future studies should refine our model to account for external factors, such as welding slag and environment factors, that compromise model performance.

## REFERENCES


Ai, Y., Lei, C., Cheng, J., & Mei, J. (2023). Prediction of weld area based on image recognition and machine learning in laser oscillation welding of aluminum alloy. Optics and Lasers in Engineering, 160, 107258.

Ajala, S., Muraleedharan Jalajamony, H., Nair, M., Marimuthu, P., & Fernandez, R. E. (2022). Comparing machine learning and deep learning regression frameworks for accurate prediction of dielectrophoretic force. Scientific Reports, 12(1), 1-17.

Al-Maadeed, S., Boubezari, R., Kunhoth, S., & Bouridane, A. (2018). Robust feature point detectors for car make recognition. Computers in Industry, 100, 129-136.

Bizhani, M., Ardakani, O. H., & Little, E. (2022). Reconstructing high fidelity digital rock images using deep convolutional neural networks. Scientific reports, 12(1), 1-14.

Chen, S., Liu, J., Chen, B., & Suo, X. (2022). Universal fillet weld joint recognition and positioning for robot welding using structured light. Robotics and Computer-Integrated Manufacturing, 74, 102279.

Cusano, C., & Napoletano, P. (2017). Visual recognition of aircraft mechanical parts for smart maintenance. Computers in Industry, 86, 26-33.

Fujiyoshi, H., Hirakawa, T., & Yamashita, T. (2019). Deep learning-based image recognition for autonomous driving. IATSS research, 43(4), 244-252.

Han, D., Liu, Q., & Fan, W. (2018). A new image classification method using CNN transfer learning and web data augmentation. Expert Systems with Applications, 95, 43-56.

He, K., Zhang, X., Ren, S., & Sun, J. (2016). Deep residual learning for image recognition. In Proceedings of the IEEE conference on computer vision and pattern recognition (pp. 770-778).

Hu, A., Wu, L., Huang, J., Fan, D., & Xu, Z. (2022). Recognition of weld defects from X-ray images based on improved convolutional neural network. Multimedia Tools and Applications, 81(11), 15085-15102.

Islam, M. T., Siddique, B. N. K., Rahman, S., & Jabid, T. (2018, October). Image recognition with deep learning. In 2018 International conference on intelligent informatics and biomedical sciences (ICIIBMS) (Vol. 3, pp. 106-110). IEEE.

Jian, B. L., Wang, C. C., Hsieh, C. T., Kuo, Y. P., Houng, M. C., & Yau, H. T. (2019). Predicting spindle displacement caused by heat using the general regression neural network. The International Journal of Advanced

Manufacturing Technology, 104, 4665-4674.

Joutou, T., & Yanai, K. (2009, November). A food image recognition system with multiple kernel learning. In 2009 16th IEEE International Conference on Image Processing (ICIP) (pp. 285-288). IEEE.

Keysers, D., Deselaers, T., Gollan, C., & Ney, H. (2007). Deformation models for image recognition. IEEE Transactions on Pattern Analysis and Machine Intelligence, 29(8), 1422-1435.

Lei, T., Huang, Y., Wang, H., & Rong, Y. (2021). Automatic weld seam tracking of tube-to-tubesheet TIG welding robot with multiple sensors. Journal of Manufacturing Processes, 63, 60-69.

Liang, F., & Zhao, Q. (2020, December). The Reliability Analysis of Welding Robots Based on Fault Tree. In 2020 International Conference on Advanced Mechatronic Systems (ICAMechS) (pp. 147-152). IEEE.

Liao, J. R., Lee, H. C., Chiu, M. C., & Ko, C. C. (2020). Semi-automated identification of biological control agent using artificial intelligence. Scientific Reports, 10(1), 1-9.

Lin, C. J., Chu, W. L., Wang, C. C., Chen, C. K., & Chen, I. T. (2020). Diagnosis of ball-bearing faults using support vector machine based on the artificial fish-swarm algorithm. Journal of Low Frequency Noise, Vibration and Active Control, 39(4), 954-967.

Liu, M., Xie, J., Hao, J., Zhang, Y., Chen, X., & Chen, Y. (2022). A lightweight and accurate recognition framework for signs of X-ray weld images. Computers in Industry, 135, 103559.

Lü, X., Xie, C., He, X., Li, S., Xu, Y., He, S., ... & Yang, X. (2022). Automatic Recognition of Multiple Weld Types Based on Structured Light Vision Sensor Using Deep Transfer Learning. IEEE Sensors Journal.

Miao, R., Jiang, Z., Zhou, Q., Wu, Y., Gao, Y., Zhang, J., & Jiang, Z. (2021). Online inspection of narrow overlap weld quality using two-stage convolution neural network image recognition. Machine Vision and Applications, 32, 1-14.

Nacereddine, N., Goumeidane, A. B., & Ziou, D. (2019). Unsupervised weld defect classification in radiographic images using multivariate generalized Gaussian mixture model with exact computation of mean and shape parameters. Computers in Industry, 108, 132-149.

Pan, H., Pang, Z., Wang, Y., Wang, Y., & Chen, L. (2020). A new image recognition and classification method combining transfer learning algorithm and mobilenet model for welding defects. IEEE Access, 8, 119951-119960.

Paoletti, M. E., Haut, J. M., Plaza, J., & Plaza, A. (2018). A new deep convolutional neural network for fast hyperspectral image classification. ISPRS journal of photogrammetry and remote sensing, 145, 120-147.

Renjun, X., Junliang, Y., Yi, W., & Mengcheng, S. (2022). Fault detection method based on improved faster R-CNN: take ResNet-50 as an example. Geofluids, 2022, 1-9.

Shang, L., Yang, Q., Wang, J., Li, S., & Lei, W. (2018, February). Detection of rail surface defects based on CNN image recognition and classification. In 2018 20th International Conference on Advanced Communication Technology (ICACT) (pp. 45-51). IEEE.

Simonyan, K., & Zisserman, A. (2014). Very deep convolutional networks for large-scale image recognition. arXiv preprint arXiv:1409.1556.

Su, J., Vasconcellos, D. V., Prasad, S., Sgandurra, D., Feng, Y., & Sakurai, K. (2018, July). Lightweight classification of IoT malware based on image recognition. In 2018 IEEE 42Nd annual computer software and applications conference (COMPSAC) (Vol. 2, pp. 664-669). IEEE.

Wang, C. C., & Zhu, Y. Q. (2021). Identification and Machine Learning Prediction of Nonlinear Behavior in a Robotic Arm System. Symmetry, 13(8), 1445.

Wang, C. C., Kuo, P. H., & Chen, G. Y. (2022). Machine learning prediction of turning precision using optimized xgboost model. Applied Sciences, 12(15), 7739.

Wang, Q., Jiao, W., Wang, P., & Zhang, Y. (2021). A tutorial on deep learning-based data analytics in manufacturing through a welding case study. Journal of Manufacturing Processes, 63, 2-13.

Xiao, M., Yang, B., Wang, S., Zhang, Z., Tang, X., & Kang, L. (2022). A feature fusion enhanced multiscale CNN with attention mechanism for spot-welding surface appearance recognition. Computers in Industry, 135, 103583.

Yang, Y., Yang, R., Pan, L., Ma, J., Zhu, Y., Diao, T., & Zhang, L. (2020). A lightweight deep learning algorithm for inspection of laser welding defects on safety vent of power battery. Computers in industry, 123, 103306.

Yu, R., Kershaw, J., Wang, P., & Zhang, Y. (2021). Real-time recognition of arc weld pool using image segmentation network. Journal of Manufacturing Processes, 72, 159-167.

Zeba, G., Dabić, M., Čičak, M., Daim, T., & Yalcin, H. (2021). Technology mining: Artificial intelligence in manufacturing. Technological Forecasting and Social Change, 171, 120971.

Zhang, Z., Liu, W., & Sun, X. (2022). Image recognition of limited and imbalanced samples based on transfer learning methods for defects in welds. Proceedings of the Institution of

Mechanical Engineers, Part B: Journal of Engineering Manufacture, 236(12), 1643-1652.
Zhao, Y., Du, H., Wang, H., Yang, C., Liu, Y., Wang, L., ... & Wang, X. (2022, August). Weld Image Recognition based on Deep Learning. In 2022 9th International Conference on Dependable Systems and Their Applications (DSA) (pp. 241-248). IEEE.

# 基於深度學習的銲接缺陷識別設備：工業應用中的比較分析和優勢評估

賴嘉宏
國立勤益科技大學 智慧自動化工程系

## 摘 要

銲接具有廣泛的應用，非破壞檢測在銲接檢測中發揮著至關重要的角色。主要用於評估銲接必須質量並檢查是否存在缺陷，但這些評估必須由經驗豐富的操作員手動進行。因此，我們制定了一種基於深度學習的設備，可以自動進行這些評估。我們用少量圖像訓練了用於銲接缺陷的神經網路模型（WDNet），並在訓練期間調整了卷積層和池化層的深度。針對銲接缺陷識別方面進行了幾個深度學習模型的評估與比較，在評估實驗中，透過本研究的模型預測準確率高達 97.8%，優於 VGG-16 和 ResNet50，呈現在工業環境中檢測銲道用於非破壞檢測應用的潛力。